

6-Methylpyridyl for Pyridyl Substitution Tunes the Properties of Fluorescent Zinc Sensors of the Zinpyr Family

Christian R. Goldsmith and Stephen J. Lippard*

Department of Chemistry, Massachusetts Institute of Technology, Cambridge, Massachusetts 02139

Received July 5, 2005

To prepare fluorescent zinc sensors with binding affinities lower than that of the parent 9-(*o*-carboxyphenyl)-2,7-dichloro-4,5-bis(bis(2-pyridylmethyl)methylaminomethyl)-6-hydroxy-3-xanthenone (ZP1), dimethylated and tetramethylated derivatives were synthesized having either two or four of the pyridyl subunits methylated at the 6-position. Like the parent ZP1, both Me₂ZP1 and Me₄ZP1 exhibit increased fluorescence in the presence of Zn²⁺. The integrated emission of Me₂ZP1 increases 4-fold in the presence of excess zinc, whereas Me₄ZP1 displays 2.5-fold enhanced fluorescence for Zn²⁺. Methylating the 6-positions of the pyridyl rings raises the dissociation constant of the sensors and lowers the pK_a values associated with the tertiary amine ligands in a systematic manner. The properties of the dimethylated Me₂ZP1 dye resemble those of ZP1, but the tetramethylated Me₄ZP1 differs greatly from ZP1 in terms of its brightness, affinity toward Zn²⁺, exchange kinetics, and metal sensitivity. Both Me₂ZP1 and Me₄ZP1 can enter HeLa cells and signal the presence of Zn²⁺. Staining caused by both dyes is punctate, with localization patterns resembling that observed for ZP1.

Introduction

Although most cellular Zn²⁺ is bound tightly by proteins, pools of less firmly bound ion are present in a variety of cells. This mobile Zn²⁺ is proposed to act as a signaling agent to mediate processes such as apoptosis,¹ gene expression,² and neurotransmission.³ A subset of glutamatergic neurons contain vesicular Zn²⁺, “puffs” of which are released into the synapse when the neurons fire.³ The precise concentrations of Zn²⁺ within the neuronal vesicles is unknown, with upper estimates ranging to the low millimolar.³ Concentrations of Zn²⁺ in the synapse are believed to reach 10–300 μM.^{3,4} The functions of these neuronal zinc stores are not understood.

Fluorescent zinc chemosensors have been developed for imaging biological Zn²⁺.^{5–7} These probes include aryl sulfonamide derivatives of 8-aminoquinoline, such as 6-methoxy-(8-*p*-toluenesulfonamido)quinoline (TSQ)⁸ and Zinquin,⁹ as

well as Zinbo-5,¹⁰ the Zinpyr (ZP) family,^{11–15} and the ZnAF molecules.^{16,17} In addition to these small molecule sensors, synthetic peptides can also signal zinc by fluorescence enhancement.^{18,19} Despite the variety of available zinc sensors, there remains much room for improvement. Many of the aryl sulfonamide sensors form 1:1 and 1:2 Zn²⁺/ligand complexes, such that it is possible for a protein-bound zinc ion to activate the change in the dye fluorescence.⁶ Other

* To whom correspondence should be addressed: E-mail: lippard@mit.edu.

- (1) Truong-Tran, A. Q.; Carter, J.; Ruffin, R. E.; Zalewski, P. D. *Biomaterials* **2001**, *14*, 315–330.
- (2) Falchuk, K. H. *Mol. Cell. Biochem.* **1998**, *188*, 41–48.
- (3) Frederickson, C. J.; Bush, A. I. *Biomaterials* **2001**, *14*, 353–366.
- (4) Bush, A. I. *Curr. Opin. Chem. Biol.* **2000**, *4*, 184–191.
- (5) Kimura, E.; Aoki, S. *Biomaterials* **2001**, *14*, 191–204.
- (6) Jiang, P.; Guo, Z. *Coord. Chem. Rev.* **2004**, *248*, 205–229.
- (7) Chang, C. J.; Lippard, S. J. *Met. Ions Life Sci.* **2006**, in press.

- (8) Frederickson, C. J.; Kasarskis, E. J.; Ringo, D.; Frederickson, R. E. *J. Neurosci. Methods* **1987**, *20*, 91–103.
- (9) Zalewski, P. D.; Forbes, I. J.; Betts, W. H. *Biochem. J.* **1993**, *296*, 403–408.
- (10) Taki, M.; Wolford, J. L.; O'Halloran, T. V. *J. Am. Chem. Soc.* **2004**, *126*, 712–713.
- (11) Walkup, G. K.; Burdette, S. C.; Lippard, S. J.; Tsien, R. Y. *J. Am. Chem. Soc.* **2000**, *122*, 5644–5645.
- (12) Burdette, S. C.; Walkup, G. K.; Spingler, B.; Tsien, R. Y.; Lippard, S. J. *J. Am. Chem. Soc.* **2001**, *123*, 7831–7841.
- (13) Burdette, S. C.; Frederickson, C. J.; Bu, W.; Lippard, S. J. *J. Am. Chem. Soc.* **2003**, *125*, 1778–1787.
- (14) Chang, C. J.; Nolan, E. M.; Jaworski, J.; Okamoto, K.-I.; Hayashi, Y.; Sheng, M.; Lippard, S. J. *Inorg. Chem.* **2004**, *43*, 6774–6779.
- (15) Chang, C. J.; Nolan, E. M.; Jaworski, J.; Burdette, S. C.; Sheng, M.; Lippard, S. J. *Chem. Biol.* **2004**, *11*, 203–210.
- (16) Hirano, T.; Kikuchi, K.; Urano, Y.; Higuchi, T.; Nagano, T. *J. Am. Chem. Soc.* **2000**, *122*, 12399–12400.
- (17) Hirano, T.; Kikuchi, K.; Urano, Y.; Nagano, T. *J. Am. Chem. Soc.* **2002**, *124*, 6555–6562.
- (18) Shultz, M. D.; Pearce, D. A.; Imperiali, B. *J. Am. Chem. Soc.* **2003**, *125*, 10591–10597.
- (19) Godwin, H. A.; Berg, J. M. *J. Am. Chem. Soc.* **1996**, *118*, 6514–6515.

sensors bind zinc to form either exclusively 1:1 complexes^{10,13,16,17,20} or a mixture of 1:1 and 2:1 species (ZP1, ZP2) that have significant fluorescence changes only when the first Zn²⁺ ion is bound.^{11,12} With some exceptions,^{20–23} these small molecule zinc sensors rely on dipicolylamine moieties to complex zinc and consequently have dissociation constants in the nanomolar range. Because these K_d values are below the hypothesized cellular Zn²⁺ concentrations, the sensors are unable to quantify biological Zn²⁺ levels. Furthermore, from the limited kinetic data it is clear that the 1:1 Zn²⁺/ligand complexes have relatively long lifetimes in solution, limiting their application in real-time imaging.^{16,17,23} The fluorescence turn-on will persist after the Zn²⁺ concentration maximizes and begins its drop to the basal level.

Cell-permeating zinc chemosensors having lower binding affinities would alleviate these problems. Probes with K_d values in the micromolar to millimolar range could be used in conjunction with the existing nanomolar K_d probes to measure the amount of Zn²⁺ in cellular and extracellular regions of interest. The reduced zinc binding affinities associated with the higher K_d values would also lead to shorter-lived Zn²⁺/ligand complexes, with higher k_{off} values.

One way to reduce the metal–ligand affinity is to introduce steric bulk near the coordinating atoms. With ligands that use pyridyl groups to bind metal ions, such as tris(2-pyridylmethyl)amine, methylating the 6-position on one or more of the rings has been demonstrated to lower the metal affinity of the resultant ligand.^{24,25} Accordingly, we prepared and characterized ZP1 derivatives, Me₂ZP1 and Me₄ZP1, which retain the 2',7'-dichlorofluorescein platform, but employ mono- and dimethylated dipicolylamine subunits instead of the simple dipicolylamine moieties to chelate zinc. The chemical, photophysical, and Zn²⁺-responsive fluorescence properties of these sensors are described in the present Article.

Experimental Section

Materials and Methods. Acetonitrile (MeCN) was dried over 3 Å molecular sieves. Ethanol (EtOH), 2',7'-dichlorofluorescein (DCF), and paraformaldehyde were purchased from Aldrich and used as received. (2-Pyridylmethyl)(6-methyl-2-pyridylmethyl)amine²⁶ and bis(6-methyl-2-pyridylmethyl)amine²⁷ were prepared as described in the literature. Calcium chloride dihydrate, magnesium chloride hexahydrate, manganese(II) chloride tetrahydrate, ferrous ammonium sulfate hexahydrate, and cobalt(II) chloride

hexahydrate were purchased from Mallinckrodt. Nickel(II) chloride hexahydrate was purchased from Strem, copper(II) sulfate pentahydrate from Baker, and zinc and cadmium chloride from Aldrich. All metal salts were used as received.

¹H and ¹³C NMR spectra were acquired on either a Varian 300 MHz or a Varian 500 MHz spectrometer and referenced to internal standards. IR spectra were collected on an Avatar 360 FTIR instrument. Melting points were measured with a Mel-Temp apparatus. The pH values of solutions were determined with an Orion glass electrode that was calibrated with three standards prior to each use. Fluorescence spectra were obtained on either a Hitachi F-3020 or a Photon Technology International fluorescence spectrophotometer. Optical spectra were acquired on a Cary 1E spectrophotometer. High-resolution mass spectrometry was performed by staff at the MIT Department of Chemistry Instrumentation Facility. Stopped-flow kinetic data were acquired on a Hi-Tech CU-61 instrument with a Xe lamp, an excitation wavelength of 505 nm, and a 455 nm filter. The KinetAsyst 3.0 program was used to operate the instrument and analyze the acquired fluorescence data. Cell images were acquired with a Nikon Eclipse TS100 microscope equipped with an RT Diagnostics camera with illumination provided by a Chiu Mercury 100 W lamp. Magnification was 40×. Fluorescence images were obtained using an FITC-HYQ filter cube (excitation 460–500 nm, band-pass 510–560 nm). The microscope was operated with Spot Advanced software.

Syntheses. **9-(*o*-Carboxyphenyl)-2,7-dichloro-4,5-bis(6-methyl-2-pyridylmethyl)(2-pyridylmethyl)methylaminomethyl)-6-hydroxy-3-xanthenone (Me₂ZP1).** (2-Pyridylmethyl)(6-methyl-2-pyridylmethyl)amine (0.241 g, 1.13 mmol) and paraformaldehyde (0.033 g, 1.1 mmol) were refluxed in 12 mL of MeCN for 30 min. DCF (0.149 g, 371 μmol) was added in 8 mL of MeCN/H₂O (1:1), and the resulting solution was heated to reflux for 24 h. The MeCN was removed under reduced pressure, and the residue was dissolved in 5 mL of EtOH and stored overnight at –25 °C to precipitate the product as a pink solid (0.165 g, 52%). Mp: 142–3 °C. ¹H NMR (CDCl₃, 300 MHz): δ 2.62 (6 H, s), 4.05 (8 H, s), 4.21 (4 H, s), 6.62 (2 H, s), 7.11 (2 H, d, $J = 7.5$ Hz), 7.24 (6 H, m), 7.38 (2 H, d, $J = 7.8$ Hz), 7.58 (2 H, m), 7.67 (4 H, m), 8.03 (1 H, d, $J = 6.9$ Hz), 8.62 (2 H, d, $J = 4.8$ Hz). ¹³C NMR (CDCl₃, 125 MHz): δ 24.12, 49.39, 59.41, 83.47, 110.15, 111.93, 120.40, 122.37, 122.64, 123.43, 124.25, 125.49, 127.24, 127.77, 130.27, 133.79, 135.39, 137.33, 137.66, 148.92 (overlapping peaks), 151.84, 156.04, 157.08, 157.77, 157.94, 169.13. FTIR (KBr, cm⁻¹): 3409 (m), 3053 (m), 3018 (m), 2925 (m), 2811 (m), 1752 (s), 1627 (m), 1594 (s), 1579 (m), 1475 (s), 1460 (s), 1434 (s), 1368 (m), 1287 (s), 1249 (s), 1214 (s), 1157 (m), 1113 (w), 1098 (s), 1038 (w), 1016 (w), 999 (m), 977 (m), 957 (w), 891 (m), 872 (m), 796 (m), 758 (s), 701 (m). HRMS (ESI) Calcd MH⁺, 851.2510 (major), 853.2498; found, 851.2528 (major), 853.2551.

9-(*o*-Carboxyphenyl)-2,7-dichloro-4,5-bis(bis(6-methyl-2-pyridylmethyl)methylaminomethyl)-6-hydroxy-3-xanthenone (Me₄ZP1). Bis(6-methyl-2-pyridylmethyl)amine (0.146 g, 642 μmol) and paraformaldehyde (0.019 g, 633 μmol) were heated to reflux in 3 mL of MeCN for 30 min. DCF (0.090 g, 224 μmol) was added in 6 mL of MeCN/H₂O (1:1), and refluxing was continued for 24 h. The MeCN was stripped. The residue was dissolved in 2 mL of EtOH and cooled to –25 °C to precipitate the product as a pink solid (0.036 g, 18%). Mp: 183–4 °C (dec). ¹H NMR (CDCl₃, 300 MHz): δ 2.59 (12 H, s), 3.97 (8 H, s), 4.17 (4 H, s), 6.60 (2 H, s), 7.03 (4 H, d, $J = 12.5$ Hz), 7.19 (5 H, m), 7.55 (4 H, t, $J = 12.5$ Hz), 7.66 (2 H, m), 8.02 (2 H, d, $J = 11.5$ Hz). ¹³C NMR (CDCl₃, 125 MHz): δ 24.18, 49.44, 59.47, 83.47, 110.08, 111.92, 120.41, 122.34, 124.26, 125.47, 127.23, 127.71,

- (20) Henary, M. M.; Fahrni, C. J. *J. Phys. Chem. A* **2002**, *106*, 5210–5220.
 (21) Aoki, S.; Kaido, S.; Fujioka, H.; Kimura, E. *Inorg. Chem.* **2003**, *42*, 1023–1030.
 (22) Nolan, E. M.; Lippard, S. J. *Inorg. Chem.* **2004**, *43*, 8310–8317.
 (23) Nolan, E. M.; Jaworski, J.; Okamoto, K.-I.; Hayashi, Y.; Sheng, M.; Lippard, S. J. *J. Am. Chem. Soc.* **2005**, *127*, 16812–16823.
 (24) Anderegg, G.; Hubmann, E.; Podder, N. G.; Wenk, F. *Helv. Chim. Acta* **1977**, *60*, 123–140.
 (25) Shiren, K.; Fujinami, S.; Suzuki, M.; Uehara, A. *Inorg. Chem.* **2002**, *41*, 1598–1605.
 (26) Fischer, A.; King, M. J.; Robinson, F. P. *Can. J. Chem.* **1978**, *56*, 3059–3067.
 (27) Nagao, H.; Komeda, N.; Mukaida, M.; Suzuki, M.; Tanaka, K. *Inorg. Chem.* **1996**, *35*, 6809–6815.

Properties of Methylated Zinpyr-1 Fluorescent Zinc Sensors

130.25, 135.39, 137.60, 148.88, 151.91, 156.01, 157.06, 157.99, 169.16. FTIR (KBr, cm^{-1}): 3508 (m), 3431 (m), 3060 (m), 2921 (s), 2869 (m), 2826 (m), 1967 (w), 1763 (s), 1623 (m), 1592 (s), 1577 (s), 1461 (s), 1437 (s), 1370 (m), 1283 (m), 1210 (w), 1097 (w), 1038 (w), 867 (w), 785 (w), 697 (w). HRMS (ESI) Calcd (MNa)⁺, 901.2659 (major), 902.2674, 903.2632, 904.2652, 905.2634; found, 901.2659 (major), 902.2688, 903.2601, 904.2669, 905.2629.

Spectroscopic Methods. Aqueous solutions were prepared with Millipore water. Stock solutions of the dyes in DMSO were prepared, separated into aliquots, stored at $-25\text{ }^{\circ}\text{C}$, and thawed in the dark immediately before use. All spectroscopic data were collected in a pH 7.0 buffer solution of 50 mM piperazine-*N,N'*-bis(2-ethanesulfonic acid) (PIPES) and 100 mM KCl at room temperature ($22\text{ }^{\circ}\text{C}$) unless noted otherwise. Quantum yields were measured relative to fluorescein in 0.1 M NaOH ($\Phi = 0.95$)²⁸ in a manner described previously.¹² Emission was integrated from 450 to 650 nm for the quantum yield measurements. A 50 μL aliquot of 10 mM ZnCl_2 in H_2O was added to a 1.0 μM solution of dye in 3 mL of buffer to generate the fully zinc-loaded complex for its quantum yield measurement.

To measure the K_d value of $\text{Me}_4\text{ZP1}$, aliquots of 1.0 mM ZnCl_2 were added to 0.5 μM solutions of $\text{Me}_4\text{ZP1}$, which were made rigorously metal-free with Chelex resin as described previously.¹⁸ After equilibrating for 5 min, the fluorescence intensity was measured. The full data set was then analyzed with the singular decomposition value program Specfit. The K_d value of $\text{Me}_2\text{ZP1}$ was measured by a fluorescence titration as described previously.¹¹

pK_a values were measured by plotting the integrated area of the fluorescence emission spectrum against pH, recorded in the range from pH 12.5 to 1.5. A 0.5 μM solution of dye containing 11 mM KOH and 100 mM KCl was made. Its pH and fluorescence spectrum were measured. The pH was then lowered gradually by addition of HCl solutions as described previously.¹² Emission for both $\text{Me}_2\text{ZP1}$ and $\text{Me}_4\text{ZP1}$ was integrated from 515 to 700 nm. The integrated emission areas were plotted against pH and fit to the nonlinear model previously reported.¹²

Stopped-flow kinetic experiments were conducted to examine the reaction of 0.5 μM dye with an excess of ZnCl_2 in PIPES buffer. All kinetic runs were monitored to at least five half-lives. Five different concentrations of ZnCl_2 between 25 and 400 μM were used to obtain second-order rate constants for the first Zn^{2+} binding event at $4.3\text{ }^{\circ}\text{C}$. At least five data points were obtained at each concentration. To calculate activation parameters, the reaction of 25 μM ZnCl_2 with 0.5 μM of each probe was run at five temperatures ranging from 4.3 to $20.6\text{ }^{\circ}\text{C}$. At least five data points were acquired at each temperature, and the full set of data was collected twice to ensure reproducibility.

Cell Imaging. HeLa cells were plated onto sterilized glass coverslips and grown to 50% confluence in Dulbecco's modified Eagle's medium (DMEM) supplemented with 10% bovine serum, $1\times$ penicillin/streptomycin, and 2 mM L-glutamine at $37\text{ }^{\circ}\text{C}$. Aliquots of DMSO solutions of the dye were added such that the well concentration reached 5 μM . The cells were incubated at $37\text{ }^{\circ}\text{C}$ for 2 h. The DMEM was removed, and the cells were washed twice with phosphate-buffered saline (PBS). The cells were immersed in fresh DMEM with 50 μM ZnCl_2 in H_2O and 100 μM sodium pyruvate in DMSO. After 10 min of further incubation, the DMEM was removed and the cells were washed twice with PBS and imaged.

Scheme 1

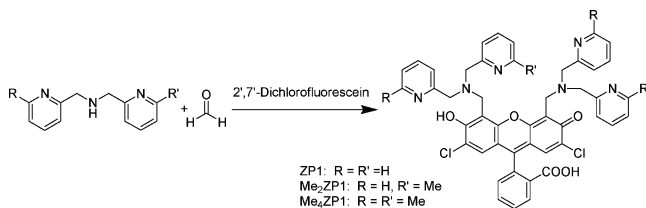


Table 1. Spectroscopic Data for ZP1, $\text{Me}_2\text{ZP1}$, and $\text{Me}_4\text{ZP1}$ ^a

compound	absorption		emission	
	λ_{max} (nm)	ϵ ($\text{M}^{-1}\text{ cm}^{-1}$)	λ_{max} (nm)	Φ^c
Apo-ZP1 ^b	515	79500	531	0.39
$\text{Zn}_2\text{-ZP1}^b$	507	78000	527	0.87
Apo- $\text{Me}_2\text{ZP1}$	515	74300	528	0.18
$\text{Zn}_2\text{-Me}_2\text{ZP1}$	505	80600	524	0.61
Apo- $\text{Me}_4\text{ZP1}$	516	56000	529	0.17
$\text{Zn}_2\text{-Me}_4\text{ZP1}$	506	47400	525	0.35

^a All measurements taken in 50 mM PIPES, 100 mM KCl, pH 7.0 buffer at RT. ^b Ref 11.

Results

Syntheses. The two ligands were prepared in one step from their respective secondary amines (Scheme 1)^{26,27} in a manner similar to the synthesis of ZP1 by a Mannich reaction with 2',7'-dichlorofluorescein (DCF).¹¹ The products precipitated from EtOH solutions were pure without the need for chromatography. The isolated solids are indefinitely stable, although stock solutions in DMSO discolor over days unless kept frozen.

Photophysical Properties. Table 1 summarizes the photophysical properties of the methylated ZP1 dyes. Upon addition of Zn^{2+} , the optical spectra of both compounds undergo slight changes. The wavelength of maximum absorption (λ_{max}) lowers by 10 nm with less than a 20% change in the intensity. The fluorescence intensities of both $\text{Me}_2\text{ZP1}$ and $\text{Me}_4\text{ZP1}$, conversely, increase dramatically upon addition of Zn^{2+} . The overall emission is enhanced 4-fold for $\text{Me}_2\text{ZP1}$ and 2.5-fold for $\text{Me}_4\text{ZP1}$ (Figure 1).

Dissociation Constants. The dissociation constant (K_d) of each compound was calculated by analyzing titrations of ZnCl_2 to each dye, using fluorimetry to monitor changes in emission. The K_d value for $\text{Me}_2\text{ZP1}$ was determined by the methodology and buffer system used for ZP1 and ZP2 (Figure S1 in the Supporting Information).¹² The K_d value for $\text{Me}_4\text{ZP1}$ is too high to be measured using the reported mixed-metal buffer system and was instead calculated from a direct titration of ZnCl_2 to a rigorously metal-free solution of dye (Figure S2 in the Supporting Information); this procedure has been used in the analysis of fluorescent peptides having similar zinc affinities.¹⁸ The data were analyzed by the singular value decomposition program Specfit. As anticipated, both ligands have lowered affinities toward Zn^{2+} relative to previously synthesized ZP ligands. $\text{Me}_2\text{ZP1}$ has a K_d value corresponding to the first zinc binding event of $3.3 (\pm 0.2)$ nM, only slightly higher than the 0.7 nM value for the parent ZP1.¹² $\text{Me}_4\text{ZP1}$ has an analogous K_d value of $630 (\pm 50)$ nM, much higher than those of either ZP1 or $\text{Me}_2\text{ZP1}$.

(28) Brannon, J. H.; Magde, D. *J. Phys. Chem.* **1978**, *82*, 705–709.

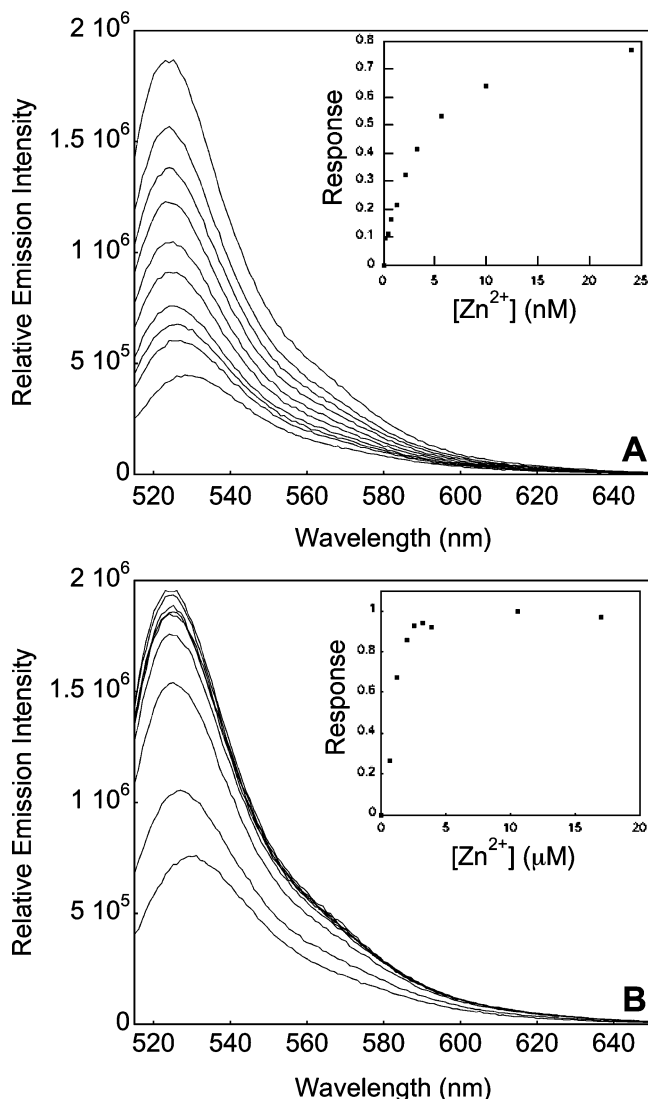


Figure 1. Fluorescence enhancement of methylated ZP1 probes upon addition of Zn^{2+} solutions at pH 7.0 in 100 mM KCl, 50 mM PIPES. (A) The concentration of $\text{Me}_2\text{ZP1}$ is $0.5 \mu\text{M}$, and the concentrations of free Zn^{2+} increase to reach 0.0, 0.42, 0.79, 1.3, 2.1, 3.4, 5.6, 10.2, 24, and 25 000 nM. (B) The concentration of $\text{Me}_4\text{ZP1}$ is $0.5 \mu\text{M}$, and the concentrations of added Zn^{2+} increase to reach 0.0, 0.67, 1.33, 2.00, 2.66, 3.32, 3.98, 10.6, and $17.0 \mu\text{M}$.

pH-Dependent Behavior. The apparent $\text{p}K_a$ values were measured by analyzing plots of integrated fluorescence versus pH (Figure 2) and are listed in Table 2. Both $\text{Me}_2\text{ZP1}$ and $\text{Me}_4\text{ZP1}$ show an initial two-step increase in fluorescence as the pH is lowered, corresponding to the two highest $\text{p}K_a$ values. With regard to this property, both dyes differ from ZP1, which displays a single-step increase in fluorescence at pH 8.37.¹² The emission begins to diminish below pH 3. The drop in intensity for both compounds is best modeled by a single step and corresponds to the lowest $\text{p}K_a$ values listed in Table 2. It should be noted that the lowest $\text{p}K_a$ values are estimates, since complete fluorescence turn-off was not achieved during the titrations. Each of the three apparent $\text{p}K_a$ values for $\text{Me}_4\text{ZP1}$ is lower than the corresponding value for $\text{Me}_2\text{ZP1}$.

Kinetics of Zn^{2+} Binding. For $\text{Me}_2\text{ZP1}$ and $\text{Me}_4\text{ZP1}$, there is a linear correlation between the pseudo-first-order rate

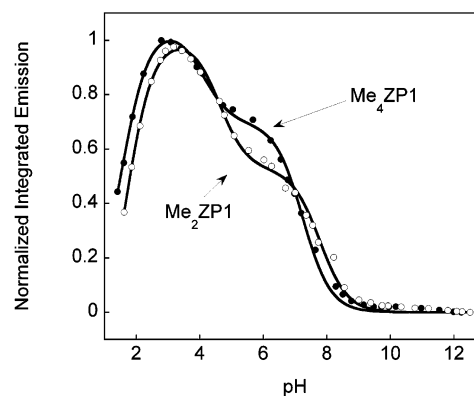


Figure 2. Normalized integrated emission vs pH for $\text{Me}_2\text{ZP1}$ and $\text{Me}_4\text{ZP1}$. The fit to the model (ref 12) is shown for each compound. The best fit $\text{p}K_a$ values are listed in Table 2.

constant and the concentration of excess Zn^{2+} (Figures S3 and S4 in the Supporting Information), and the overall reaction is most simply interpreted as a second-order reaction, first-order in both zinc and probe. The second-order rate constants for the addition of the first equiv of Zn^{2+} to the ligands are denoted k_{on} and given in Table 2. The first-order rate constants for the dissociation of Zn^{2+} from the 1:1 resultant complex, calculated from the K_d values and the second-order rate constants, are denoted k_{off} (Table 2). The complexation reactions for both methylated dyes proceed more slowly than those for ZP1,²³ with $\text{Me}_2\text{ZP1}$ being 4-fold more reactive than $\text{Me}_4\text{ZP1}$. The zinc dissociation reaction associated with k_{off} proceeds most rapidly with $\text{Me}_4\text{ZP1}$. Unexpectedly, the dissociation of zinc from $\text{Me}_2\text{ZP1}$ is 6-fold slower than zinc loss from ZP1.

Metal Ion Competition Studies. Metal ion selectivity assays were performed for both $\text{Me}_2\text{ZP1}$ and $\text{Me}_4\text{ZP1}$ as previously described.¹⁴ The dyes were first added to a solution of $50 \mu\text{M}$ M(II) in buffer, where $\text{M} = \text{Ca}, \text{Mg}, \text{Mn}, \text{Fe}, \text{Co}, \text{Ni}, \text{Cu},$ or Cd . Of these metal ions, only Cd^{2+} enhances the fluorescence (Figure 3). The alkaline-earth metals Ca^{2+} and Mg^{2+} do not diminish the Zn^{2+} -induced emission, even when present in great excess (5 mM). The first-row transition metal ions Mn^{2+} , Fe^{2+} , Co^{2+} , Ni^{2+} , and Cu^{2+} reduce the fluorescence intensity. With the exception of Mn^{2+} , these ions interfere with the ability of $50 \mu\text{M}$ of Zn^{2+} to turn on the sensor fully. With $\text{Me}_2\text{ZP1}$, essentially no fluorescence enhancement occurs upon Zn^{2+} addition to solutions containing Fe^{2+} , Co^{2+} , Ni^{2+} , and Cu^{2+} . With $\text{Me}_4\text{ZP1}$, integrated emission significantly increases following Zn^{2+} addition to both the Fe^{2+} and the Ni^{2+} solutions after 1 min. After 1 h, the integrated fluorescence for mixed solutions containing Fe^{2+} and Co^{2+} increases, although the emission for the solution containing Co^{2+} does not approach that of the metal-free dye. The fluorescence of the Ni^{2+} solution drops to the pre- Zn^{2+} addition level over 1 h. The solution containing Cu^{2+} fluoresces the most weakly, and its emission does not change appreciably at either 1 min or 1 h after Zn^{2+} addition.

Cell Studies. The cell permeabilities of the methylated ZP1 sensors were assayed in HeLa cells (Figure 4). After incubation with $5 \mu\text{M}$ of the dye, the cells display

Table 2. Dissociation Constants, pK_a Values, and Rate Constants for ZP1, Me₂ZP1, and Me₄ZP1

compound	first K_d (nM) ^a	pK_a	k_{on} (M ⁻¹ s ⁻¹) ^{b,c}	k_{off} (s ⁻¹) ^{b,d}
ZP1 ^e	0.7 (±0.1)	2.75, 8.37 ^f	3.3×10^6	2.3×10^{-3}
Me ₂ ZP1	3.3 (±0.2)	1.7, 4.78, ^f 7.78 ^f	$1.13 (\pm 0.05) \times 10^5$	$4.00 (\pm 0.25) \times 10^{-4}$
Me ₄ ZP1	630 (±50)	1.5, 4.09, ^f 7.25 ^f	$2.53 (\pm 0.25) \times 10^4$	$1.59 (\pm 0.20) \times 10^{-2}$

^a Measurements taken in 50 mM PIPES, 100 mM KCl, pH 7.0 buffer at RT. ^b Measurements taken in 50 mM PIPES, 100 mM KCl, pH 7.0 buffer at 4.3 °C. ^c Second-order rate constant for the addition of the first equiv of Zn²⁺ to the sensor. ^d First-order rate constant for the dissociation of Zn²⁺ from the 1:1 Zn²⁺/ligand complex. ^e Refs 11 and 23. ^f pK_a values associated with the PET switching in the zinc-responsive probes. This process is believed to correlate to the protonation of the tertiary amine nitrogens.

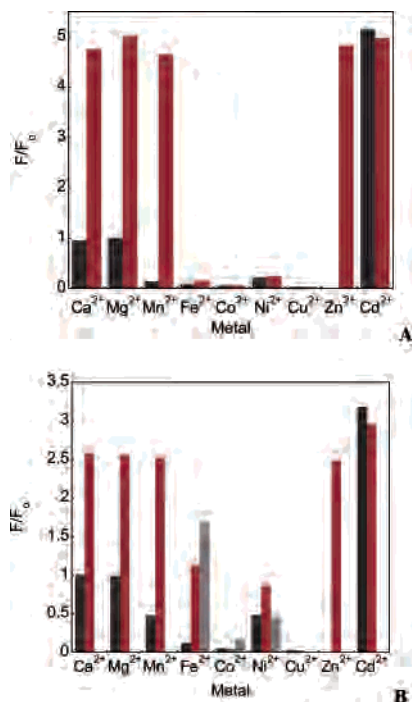


Figure 3. Metal ion selectivity assays for Me₂ZP1 (A) and Me₄ZP1 (B). The first bar (dark gray) is the fluorescence response of 0.5 μ M of the probe to 50 μ M of the metal ion at pH 7.0 in 100 mM KCl, 50 mM PIPES. The second bar (red) is the fluorescence response after the addition of 50 μ M ZnCl₂, after allowing 1 min for equilibration. The third bar (light gray) is the fluorescence response after the addition of 50 μ M ZnCl₂ to the solutions containing 50 μ M Fe(II), Co(II), Ni(II), and Cu(II), after allowing 60 min for equilibration. The response is normalized to the fluorescence of the free dye (F_0).

modest intracellular staining, indicating that Me₂ZP1 and Me₄ZP1 are both cell permeable. The cells become noticeably more fluorescent when 50 μ M ZnCl₂ and 100 μ M pyrithione are added, the latter to facilitate Zn²⁺ diffusion into the cell. Subsequent addition of the cell-permeable metal chelator *N,N,N',N'*-tetrakis(2-pyridylmethyl)ethylenediamine (TPEN) quenches the emission (data not shown), consistent with intracellular turn-on being a consequence of reversible zinc binding.

Discussion

Biologically relevant concentrations of mobile Zn²⁺ are estimated to range from ~ 1 fM²⁹ in *E. coli* to ~ 0.5 mM in mammalian cells.^{3,4} Sensors with a wide range of binding affinities are therefore desired in order to monitor this form of Zn²⁺ in biology. Many of the available probes, such as ZP1, rely on dipicolylamine subunits to chelate zinc and form

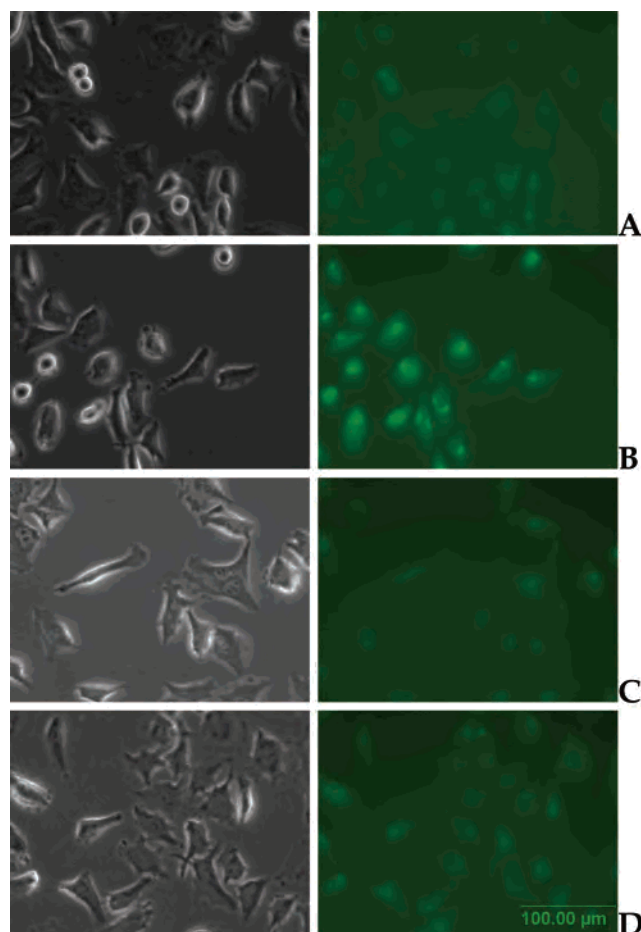
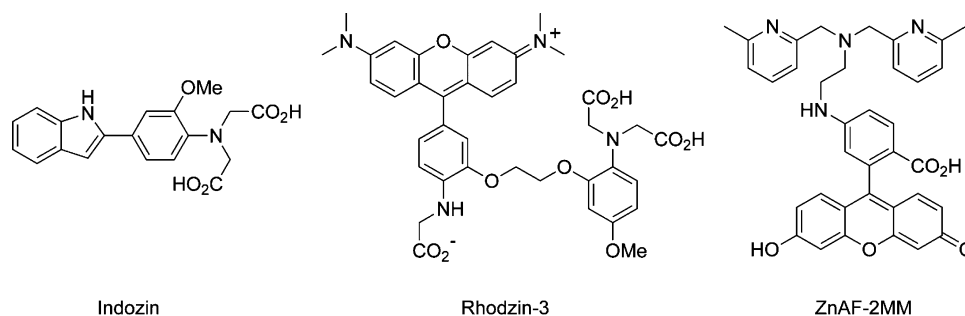


Figure 4. Phase contrast (left) and fluorescence microscopy (right) images of HeLa cells treated with 5 μ M methylated ZP1 for 2 h at 37 °C. (A) Cells treated with Me₂ZP1, with no ZnCl₂ or pyrithione added. (B) Cells treated with Me₂ZP1, with 50 μ M ZnCl₂ and 100 μ M pyrithione added. Cells were incubated an additional 30 min after zinc addition and rinsed with PBS prior to imaging. (C) Cells treated with Me₄ZP1, with no ZnCl₂ or pyrithione added. (D) Cells treated with Me₄ZP1, with 50 μ M ZnCl₂ and 100 μ M pyrithione added. Cells were incubated an additional 10 min after zinc addition and rinsed with PBS prior to imaging.

1:1 Zn²⁺/ligand complexes with K_d values of ~ 1 nM.^{10,12–14,16,17} Although these probes are valuable for qualitatively detecting the presence of Zn²⁺ in most biological media, they are less well suited to study mobilization of the elevated Zn²⁺ levels found in the presynaptic vesicles of the dentate gyrus region of the hippocampus.^{3,4} To reduce the affinity of a ligand for a metal, one can either weaken the individual metal–ligand bonds or decrease their number. The latter approach was employed by us in the design of the QZ²³ and Zinspy dyes,²² reported elsewhere, where eliminating one of the binding arms raised the K_d value to ~ 10 μ M. In the present work, we attenuated the ligand binding affinity by adding steric

(29) Outten, C. E.; O'Halloran, T. V. *Science* **2001**, 292, 2488–2492.

Scheme 2



bulk near the coordinating atoms. Such a perturbation lengthens and thereby weakens the metal–ligand bonds. The ZP1 derivatives, Me₂ZP1 and Me₄ZP1 (Scheme 1), are manifestations of this design principle in which methyl groups are installed at the 6-positions of the pyridine rings. This modification affects the structure of metal complexes with tris(2-pyridylmethyl)amine derivatives and destabilizes them relative to complexes with the unmodified ligand.^{24,25} During the preparation of this manuscript, methylated versions of the zinc sensor ZnAF-2 were reported; the resultant ZnAF-2M and ZnAF-2MM probes similarly form weaker complexes with Zn²⁺.³⁰

Like ZP1, both Me₂ZP1 and Me₄ZP1 exhibit enhanced fluorescence in the presence of Zn²⁺, with respective increases of 4-fold and 2.5-fold in emission intensity. In both instances, the amplification is similar to that of ZP1.¹¹ Addition of excess EDTA to solutions of the methylated ZP1 dyes and Zn²⁺ restores the fluorescence to its original level, indicating that the turn-on results from the reversible binding of Zn²⁺. Methylation of the dipicolyl subunits of ZP1 diminishes the intensity of the resultant dyes. The quantum yields of the zinc-loaded sensors drop from 0.87 (ZP1)¹¹ to 0.61 (Me₂ZP1) to 0.35 (Me₄ZP1). The quantum yields of the apo forms of the methylated ZP1 compounds are both lower than that of ZP1 as well.¹¹ Methyl groups are electron-releasing and may enhance the ability of the tertiary amines to quench the fluorescein excited state, reducing emission in both the apo and zinc-loaded forms of the ligand. The other photophysical properties of the three sensors, including the maxima of absorbance and emission, do not change significantly upon methylation. Since the parent fluorophore is 2',7'-dichlorofluorescein for all three sensors, the similarities in the photophysical properties are anticipated.

Methylation increases the K_d values of the ligands relative to that of ZP1. Incorporation of the first two methyl groups (Me₂ZP1) has a small influence on the dissociation constant associated with the first Zn²⁺ binding event, the K_d value of Me₂ZP1 being less than an order of magnitude higher than that of ZP1. The addition of the second two methyl groups has a much larger impact. Me₄ZP1, with four 6-methylpyridyl groups, has a K_d of 630 nM, nearly 3 orders of magnitude greater than that of ZP1. Among non-peptide-based sensors selective for Zn²⁺, Me₄ZP1 has a binding affinity between the ZP1 and the QZ and Zinspy analogues^{22,23} and is also

intermediate between those of IndoZin (3.0 μ M) and RhodZin-3 (65 nM).³¹ The dimethylated derivative of ZnAF-2, ZnAF-2MM, probe binds Zn²⁺ with approximately the same affinity (790 nM).³⁰ The molecular structures of these three compounds are depicted in Scheme 2.

The added methyl groups also lower the p K_a values associated with protonating the tertiary amines in the dipicolyl moieties. As the tertiary amines of ZP compounds are protonated, the fluorescence intensity of the complex increases.^{12,14} With increased methylation, the first p K_a drops from 8.37 (ZP1) to 7.78 (Me₂ZP1) to 7.25 (Me₄ZP1). The fluorescence increase for each methylated dye occurs over two separate pH-dependent events. The simplest explanation for this behavior is that protonation of the second tertiary amine in each molecule is also fluorimetrically observable, but it is unknown why this phenomenon is observed for the methylated dyes and certain ZP compounds³² but not for others.^{12,15} The second step of the fluorescence increase is associated with apparent p K_a values of 4.78 (Me₂ZP1) and 4.09 (Me₄ZP1). The emission of the sensors decreases below pH 4 and is consistent with protonation of the fluorescein carboxylate. The properties of the protonated forms of the ZP dyes qualitatively resemble those of the zinc-loaded forms, and ZP ligands that are too basic cannot signal the presence of zinc at neutral pH values. Reduced emission from the protonated dyes lowers the background fluorescence in the absence of Zn²⁺ for the methylated ZP1 probes relative to that for ZP1. The fact that a large portion of the protonation-induced turn-on occurs at a pH well below 7 contributes to the diminished background fluorescence of the methylated sensors relative to that of ZP1.

Stopped-flow kinetic studies of Me₂ZP1 and Me₄ZP1 indicate that both ligate zinc more slowly than chemosensors having chelating dipicolylamine subunits,^{16,17,23} with Me₄ZP1 reacting particularly slowly. Eyring plots encompassing data from 4.3 to 20.6 °C (Figures S5 and S6 in the Supporting Information) yield similar activation parameters for Me₂ZP1 ($\Delta H^\ddagger = 13.9 (\pm 0.1)$ kcal mol⁻¹, $\Delta S^\ddagger = 15.0 (\pm 0.5)$ cal mol⁻¹ K⁻¹) and Me₄ZP1 ($\Delta H^\ddagger = 16.1 (\pm 0.1)$ kcal mol⁻¹, $\Delta S^\ddagger = 19.9 (\pm 0.4)$ cal mol⁻¹ K⁻¹). These parameters are greater than those of nonmethylated ZP1 ($\Delta H^\ddagger = 12.5$ kcal mol⁻¹, $\Delta S^\ddagger = 13.2$ cal mol⁻¹ K⁻¹)²³ and scale with increasing

(30) Komatsu, K.; Kikuchi, K.; Kojima, H.; Urano, Y.; Nagano, T. *J. Am. Chem. Soc.* **2005**, *127*, 10197–10204.

(31) Kikuchi, K.; Komatsu, K.; Nagano, T. *Curr. Opin. Chem. Biol.* **2004**, *8*, 182–191.

(32) Woodrooffe, C. C.; Masalha, R.; Barnes, K. R.; Frederickson, C. J.; Lippard, S. J. *Chem. Biol.* **2004**, *11*, 1659–1666.

methylation. The results suggest that, within this series of related compounds, the rate of complexation depends on the strength of the initial bond formed between Zn^{2+} and the ligand. The bond between pyridyl ligands and metal ions is typically shorter and stronger than those formed with 6-methylpyridyl ligands.²⁴ A stronger initial bond would lower the activation energy if this step were rate-limiting, thereby explaining why ZP ligands with nonmethylated pyridines complex Zn^{2+} more quickly. The K_d and k_{on} values in Table 2 were used to compute k_{off} values, which reflect the stability of the 1:1 Zn^{2+} /ligand complex. The k_{off} value for $\text{Me}_2\text{ZP1}$ is less than that for ZP1, an unexpected result given the greater K_d value for $\text{Me}_2\text{ZP1}$.²³ When the concentration of Zn^{2+} drops, both zinc-loaded compounds will release the metal ion slowly. $\text{Me}_4\text{ZP1}$, conversely, has a much higher k_{off} value, and Zn^{2+} will be able to dissociate from the sensor much more readily. The faster release rate is presumably a consequence of the weaker Zn–N bonds formed with 6-methylpyridyl relative to those of the pyridyl groups. The $\text{Me}_4\text{ZP1}$ dye is thus the best suited of the three for real-time Zn^{2+} imaging, since it can respond more quickly to changes in the concentration of zinc than $\text{Me}_2\text{ZP1}$ and ZP1.

Metal ion selectivity studies revealed that Zn^{2+} was unable to generate an enhanced fluorescence response for $\text{Me}_2\text{ZP1}$ in the presence of Fe^{2+} , Co^{2+} , Ni^{2+} , or Cu^{2+} . This result parallels that observed for ZP1 under similar conditions.¹² Further studies of $\text{Me}_2\text{ZP1}$ indicate that, once the zinc complex is formed, the competing metal ions are unable to quench its induced fluorescence (Figure S7 in the Supporting Information). The Fe^{2+} , Co^{2+} , and Ni^{2+} salts have no effect, whereas Cu^{2+} leads to only a small diminution in integrated emission 1 min after the metal addition. After these other metal ions bind to $\text{Me}_2\text{ZP1}$, however, their presumably slow dissociations from the ligand will preclude even a large excess of Zn^{2+} from inducing a rapid fluorescence response. Slow metal exchange rates preclude a meaningful assessment of the true thermodynamic affinity for first-row transition metals of these fluorescent ligands, the long-term stabilities of which have not been established.

The metal ion selectivity assay results with $\text{Me}_4\text{ZP1}$ reflect its faster exchange rate. Addition of Zn^{2+} to a solution of $\text{Me}_4\text{ZP1}$ in 50 μM of the competing metal ion immediately amplifies the emission in the presence of Fe^{2+} and Ni^{2+} . After 1 h there are additional increases in the cases of Fe^{2+} and Co^{2+} , although emission for the latter never approaches that

of the free dye. With the exception of Ni^{2+} , the latter plot is more representative of the thermodynamic affinities of the metal ions for $\text{Me}_4\text{ZP1}$ predicted by the Irving–Williams series. The Cu^{2+} ion is most strongly coordinated by the ligand. Taken together, these results suggest that the increased lability associated with higher k_{off} values renders the Zn^{2+} probes less susceptible to fluorescence quenching by more weakly binding metal ions.

Methylation has no impact on the ability of the dyes to enter cells, based on preliminary studies with HeLa cells. Both $\text{Me}_2\text{ZP1}$ and $\text{Me}_4\text{ZP1}$ display enhanced intracellular fluorescence following incubation with ZnCl_2 and pyridithione. As with ZP1, the staining appears to be punctate, suggesting that the dyes aggregate in particular organelles within the cell. The fluorescence turn-on with $\text{Me}_4\text{ZP1}$ is significantly less than that for $\text{Me}_2\text{ZP1}$ (Figure 4), as expected from the photophysical properties measured *in vitro* (Table 1). The addition of one equiv of TPEN, a cell-permeable metal-sequestering agent, to the cell media diminished the emission, as anticipated from prior work.^{11,12,15,23}

Summary

The two ligands $\text{Me}_2\text{ZP1}$ and $\text{Me}_4\text{ZP1}$ have reduced affinities for Zn^{2+} and lower tertiary amine $\text{p}K_a$ values relative to those of Zinpyr-1. Methylation does not significantly alter the Zn^{2+} -induced fluorescent response, although the methylated dyes are not as bright as ZP1. Tetramethylation has a more profound impact than dimethylation on the ligand properties, particularly the K_d associated with the first zinc binding event and the rate constant for zinc release. Methylation of ZP1 does not affect the ability of the probes to traverse cell membranes and detect Zn^{2+} within cells.

Acknowledgment. This work was supported by Grant GM 65519 from the National Institute of General Medical Sciences (S.J.L.) and a postdoctoral fellowship from the National Institutes of Health (C.R.G.). We thank Dr. K. R. Barnes for her assistance with cell studies.

Supporting Information Available: Fits used to calculate dissociation constants; plots used to calculate k_{on} values; Eyring plots of the reaction between the methylated ZP1 probes and ZnCl_2 acquired within the 4.3–20.6 °C temperature range; a plot showing the emission response of $\text{Zn}_2\text{-Me}_2\text{ZP1}$ to added metal ions; sample stopped-flow kinetic data. This material is available free of charge via the Internet at <http://pubs.acs.org>.

IC051113S